On the efficient representation of comprehensive, precise spectroscopic data sets: The A state of I_2

Cite as: J. Chem. Phys. **118**, 3532 (2003); https://doi.org/10.1063/1.1539849
Submitted: 26 August 2002 . Accepted: 02 December 2002 . Published Online: 04 February 2003

Joel Tellinghuisen

On the efficient representation of comprehensive, precise spectroscopic data sets: The *A* state of I_2

Joel Tellinghuisen
Department of Chemistry, Vanderbilt University, Nashville, Tennessee 37235

(Received 26 August 2002; accepted 2 December 2002)

Mixed representations—polynomials in $(v+1/2)$ at low v, near-dissociation expansions (NDEs) in (v_D-v) at high v—are tested for their ability to fit a comprehensive and precise data set for the *A* state of I_2. The combined functions for the vibronic energy T_v and the rotational constant B_v are rendered smooth at the point of switchover through two approaches: the use of Lagrange's method of undetermined multipliers to incorporate exactly satisfied constraints for continuity in the functions and their first derivatives, and the use of a smooth switching function. As compared with a previously reported pure NDE analysis [Appadoo *et al.*, J. Chem. Phys. **104**, 903 (1996)], both approaches yield significantly reduced chi-square and a more realistic extrapolation of B_v from the highest analyzed level ($v=35$) to dissociation. The switching-function method has a number of advantages over the constraint method, and is thus recommended as the preferred approach for fitting to mixed representations. © *2003 American Institute of Physics.*
[DOI: 10.1063/1.1539849]

I. INTRODUCTION

From the dawn of quantum mechanics, diatomic molecular energies have been represented most simply in terms of the harmonic oscillator-rigid rotor model, in which the vibrational energies are proportional to $x=(v+\frac{1}{2})$ and the rotational to $\kappa=J(J+1)$. Perturbation treatments of deviations from this model naturally expressed the corrections to the energy terms of these same variables, and initially the corrections were represented in terms of a few coefficients with sometimes unwieldy labels.[1] By the early 1970s diatomic spectroscopists were fitting comprehensive data sets spanning large ranges of v to double polynomials in x and κ, with the number of terms determined empirically from the data in question.[2] However, when the range of v spanned by the data approaches the dissociation limit, the polynomials in x become inefficient for representing the vibrational dependence, requiring many terms and extra care and attention to matters concerning computational precision. For example, a 1980 analysis of the $D\rightarrow X$ fluorescence spectrum of I_2 required 15 vibrational parameters and eight rotational parameters to represent v'' levels 0–99, which covered 99.7% of the *X* state energetically.[3] A later work on this same *X* state, with much more abundant and precise data extending to $v=108$, required 15 vibrational and 15 rotational parameters for just the region 0–89, and then an additional 11 vibrational and 15 rotational parameters for the higher levels.[4]

In 1980 Le Roy and Lam pioneered the use of ''top-down'' expressions for representing diatomic spectroscopic constants in terms of the theoretically predicted behavior of these properties in the dissociation limit.[5] In this approach the constants are given by ''near-dissociation expansions'' (NDEs), in which the argument is $y=(v_D-v)$, with v_D being the (noninteger) value of the vibrational quantum number at dissociation. Deviations from limiting behavior are accommodated by various empirical functions of y, including polynomials, exponential polynomials, and rational polynomials. These NDEs are far more efficient in the high-v region, and have been used to represent the full range of observed levels, in some cases extending down to $v=0$.[6–22] In one such study, key to the present work, Appadoo *et al.*[16] examined the performance of both polynomials and NDEs in fitting a large, precise data set covering $v=0-35$ of the *A* $(1_u\ {}^3\Pi)$ state of I_2. Their comparisons came down solidly in favor of NDEs.

In addition to their high efficiency, NDEs are touted for their superior interpolating and extrapolating ability across regions not covered by experimental data. However, they can misbehave, especially as the orders of the correction functions become large.[7] For example, Fig. 1 shows that the NDE for B_v from Appadoo *et al.*,[16] which contains 12 adjustable parameters, exhibits an improbable behavior in the region between the highest observed level and the dissociation limit. On the other hand, the dashed curve, which is computed from a six-term NDE obtained as discussed below, displays a more reasonable behavior in this region.

Some time ago, we suggested that one can reap the best and avoid the worst from polynomials and NDEs by simply fitting the data to both simultaneously—polynomials at low v and NDEs at high.[24–26] From the several cases examined, we concluded that the traditional polynomials in $(v+\frac{1}{2})$ were optimal for about the lowest third of the v levels (covering about $\frac{2}{3}$ of the potential well energetically) and NDEs for the remaining two-thirds. The number of parameters needed to represent the data adequately was about the same as for either pure representation, but the fitting was actually easier, because the coefficients of the two functions were not highly correlated. Also, since both functions were now of lower order, their extrapolating ability was better. Furthermore, the polynomials gave directly the important equilibrium constants, T_e, ω_e, B_e, and their errors. The one added compli-

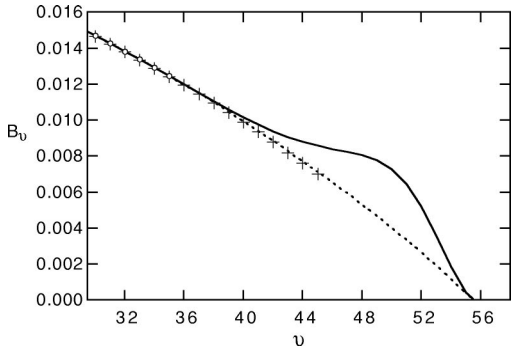

FIG. 1. B_v (cm^{-1}) at high v for the A state of I_2. Circles indicate levels included in the experimental data analyzed in Ref. 16, while the solid curve is the prediction of the rotational NDE from that study. The + symbols are values determined by Yukiya *et al.* (Ref. 23). The dashed curve is from the present analysis by mixed polynomial/NDE representations (MXRs).

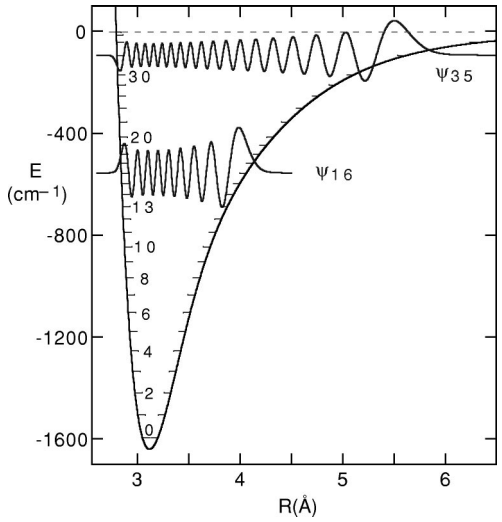

FIG. 2. Potential curve for the A state of I_2, referenced to the dissociation limit 12 547.354 cm^{-1} above the minimum of the X state. Wave functions are shown for the highest analyzed v level in Ref. 16 and for the level that is optimal for switchover in the MXR fits of the present work.

cation was the need to impose smoothness constraints, which we did by using Lagrange's method of undetermined multipliers to require that T_v and B_v and their first derivatives be continuous at the switchover point (v_S). Since the constraints are exactly satisfied in this method, this effectively decreased the number of free parameters by four. However, the resulting variance penalty was a modest ~1%.

The previous tests of this mixed fitting approach involved data sets that were either sparse or imprecise, or both. The analysis by Appadoo *et al.*[16] of an extensive (9552 lines) and precise (0.005 cm^{-1}) data set lays the groundwork for a much more instructive test of this method, and that is the subject of this paper. In the following sections, I describe the results obtained using both the original approach of constrained fitting, and an appealing alternative of a smooth switching function. Both methods easily better the precision of the Appadoo NDE, yielding a chi-square as much as 30% smaller. This is found to be due mainly to reduced systematic error in the low-v region. At the same time, the extrapolating ability at high v is better, as shown in Fig. 1, and, as already noted, the fitting is easier. In fact, I was able to achieve most of the results presented below working in double precision (64 bits) and using the ''lazy'' approach to nonlinear least-squares fitting: Define the fit function in a function routine and let the program take all required derivatives numerically.[27] The best fits did require more adjustable parameters than the 26 of the Ref. 16 NDE—8 more in the case of the examples summarized below. However, because the fit parameters are less correlated, the number of decimal digits needed to summarize these results is essentially the same as required for the Appadoo NDE.

For reference, Fig. 2 illustrates the potential curve for the A state of I_2, with wave functions shown for the highest level analyzed in Ref. 16 and for the level that turns out to be the optimal switchover level for the mixed-representation (MXR) fits.

II. THEORY AND COMPUTATIONAL METHODS

A. Nonlinear least-squares with constraints

The mathematics of constrained fitting was treated in Refs. 24 and 25 and will be reviewed only briefly here. If S represents the sum of weighted, squared residuals, then the least-squares (LS) equations are normally obtained by setting the partial derivatives of S with respect to each adjustable parameter equal to zero. if there are constraints, expressed in terms of the adjustable parameters $\boldsymbol{\beta}$ as $G_k(\boldsymbol{\beta})=0$, we subtract $\alpha_k(\partial G_k/\partial\beta_j)$ from each equation, for each constraint, where α_k is the Lagrange multiplier for the kth constraint. Thus, for example, if there are two constraints, $G_1=0$ and $G_2=0$, the equation for the jth parameter is obtained from

$$\frac{\partial S}{\partial \beta_j}-\alpha_1\frac{\partial G_1}{\partial \beta_j}-\alpha_2\frac{\partial G_2}{\partial \beta_j}=0. \tag{1}$$

In nonlinear fitting, the least-squares equations are solved iteratively.[28,29] With constraints included, each iteration involves (1) solving for the multipliers α, and (2) using these values to compute the adjustments to the estimates of the parameters $\boldsymbol{\beta}$. The computations proceed until some convergence criterion is satisfied. In the methods commonly used to implement the iterative algorithm, the matrix $\mathbf{A}=\mathbf{X}^\mathbf{T}\mathbf{W}\mathbf{X}$ is computed and inverted. The elements of $\mathbf{X}$ are the partial derivatives of the fit function with respect to the parameters, evaluated at the ith data point, $X_{ij}=(\partial F/d\beta_j)_i$. The weight matrix $\mathbf{W}$ is diagonal, of dimension equal to the number of data points, with elements w_i.

In linear LS, under the usual assumptions of unbiased, normally distributed data, the parameter variances are the diagonal elements of the variance-covariance matrix $\mathbf{V}$, which is proportional to $\mathbf{A}^{-1}$. If we assume that the statistical data errors σ_i are known, and define the weights as $w_i=\sigma_i^{-2}$, then $\mathbf{V}=\mathbf{A}^{-1}$, and S is an estimate of chi-square for the fit. If the fit model is correct, χ^2 should be about equal to the number of degrees of freedom ν, which is the number of data points minus the number of adjustable parameters. Equivalently, the reduced chi-square, $\chi^2_\nu=\chi^2/\nu$, should be about 1. In the alternative view that the data errors are unknown or known only in a relative sense (which is more often the approach taken in physical science), S/ν becomes

an estimate of σ_{y1}^2, the variance for data of unit weight. Then $\mathbf{V}=\sigma_{y1}^2\mathbf{A}^{-1}$. In those cases where the data error is *thought* to be known, but χ_ν^2 differs significantly from unity, the conservative approach is to take the larger of the two possible estimates of $\mathbf{V}$.[30] This means $\mathbf{V}=\mathbf{A}^{-1}$ if $\chi_\nu^2<1$ and $\mathbf{V}=\chi_\nu^2\mathbf{A}^{-1}$ if >1. Where parameter standard errors are reported below, this approach is used.

In nonlinear LS, much of the above is not rigorously true, and nonlinear parameters may not even have a defined variance.[31] However, as long as the statistical errors are relatively small, say $<10\%$ of the parameter values, the asymptotic error estimates remain useful predictors of the parameter distributions. These estimates are obtained exactly as above, for both constrained and unconstrained (normal) nonlinear LS fitting.

Errors in functions of the parameters are calculated from the full expression for the propagation of error for correlated variables.[32] If $H=H(\boldsymbol{\beta})$, then

$$\sigma_H^2=\mathbf{h^T V h}, \tag{2}$$

where the ith element of $\mathbf{h}$ is $(\partial H/\partial\beta_i)$. Quantities of interest include the spectroscopic parameters T_v and B_v, the RKR potential, and the quantum-mechanically computed estimates of T_v, B_v, and the centrifugal distortion constants, all of which are functions of v.[33]

B. Computational approach

To keep this test simple and clean, I have treated the data exactly as done by Appadoo *et al.*, except for the use of MXRs in place of NDEs for T_v and B_v. Accordingly, for most of the computations I have used their final reported expressions and values for all the centrifugal distortion constants [CDCs, D_v, H_v, etc., represented as $K_m(v)$, $m=2-7$ in Ref. 16], including the empirically defined K_7 and its coefficient k_7. For the NDE segments of B_v and T_v, I used the same exponential polynomial correction function for B_v, and a simple polynomial (rather than the rational polynomial of Ref. 16) for T_v. Thus, these NDEs were (in terms of $y=v_{\mathcal{D}}-v$)

$$B_v=X_1y^{4/3}\mathcal{F}_B, \tag{3}$$

and

$$T_v=\mathcal{D}-X_0y^{10/3}\mathcal{F}_G, \tag{4}$$

with

$$\mathcal{F}_B=\exp\left(\sum_{i=1} p_i^1y^i\right), \tag{5}$$

and

$$\mathcal{F}_G=1+\sum_{i=2} p_iy^i. \tag{6}$$

Values for the constants X_1, X_0, and $\mathcal{D}$ were also taken from Ref. 16. In one other deviation from the model of Appadoo, I found that a third coefficient was justified for the Ω-doubling constant, which was thus expressed as a quadratic function of $(v+\frac{1}{2})$ for the full range of v.

In the constrained fitting, the four constraints are the requirements that the polynomial and NDE for each of T_v and B_v agree in value and slope at some chosen switchover $v\equiv v_S$. The alternative approach explored for the first time here is the use of a switching function to accomplish this task. I have achieved good success with the simple hyperbolic-tangent-type function

$$\mathcal{F}_S=[1+\exp(a(v-v_S))]^{-1}, \tag{7}$$

and have experimented with no others in this work. Letting, for example, B_{vp} represent the polynomial expression for B_v, and B_{vlr} the long-range expression, the fitted quantity becomes

$$B_v=\mathcal{F}_S(B_{vp}-B_{vlr})+B_{vlr}. \tag{8}$$

In this approach, the required coding beyond that needed for just NDE fitting is trivial, whereas a modicum of effort is required to implement the constraint procedure.

As was noted earlier, most of the results discussed here were obtained by simply defining the relations among the data variables and the fit parameters in a function routine and estimating the derivatives numerically. The advantage of this method is operator convenience and efficiency, as there are nonlinear driver routines readily available and easy to use.[29,34] Most of the coding work is just that needed to get the data into the program and the results out. The disadvantage is numerical instability if the derivatives are not obtained with sufficient precision. Most of the computations utilized double precision and part in 10^6 or 10^7 changes (central) to estimate the derivatives. Quadruple precision and parameter changes 10^3 times smaller were used in some of the error propagation calculations, to check the double precision results.

The numerical RKR, Schrödinger, and perturbation computations employed standard techniques, like those used by Appadoo *et al.*,[16] but independently devised.[33,35,36] An integration mesh size of 0.0005 Å was used to generate the numerical wave functions and compute the CDCs.

III. RESULTS AND DISCUSSION

Initially, subsets of the data from $v=0$ up were fitted to polynomials in $(v+\frac{1}{2})$, while subsets from $v=35$ down were fitted to NDEs. These fits were used to determine the numbers of parameters needed to represent the data with either representation separately, and to obtain initial values of the parameters for the MXR fitting. As bands were added one by one to the data set, these fits also revealed some sharp increases in chi-square for the bands containing R and P lines (see below).[37] For v_S in the range 15–21, 8–10 polynomial coefficients were needed for both T_v and B_v, while about six correction parameters were needed in the NDEs for each function. Convergence was easily achieved when the full data set was then fitted to the combined functions with constraints (MXCs). By repeating the MXC fits for various v_S, I found absolute minimum variance near $v_S=16$. The switching-function fits (MXS) were then initiated with final results from the MXC fits and again readily converged. The parameter a in Eq. (7) was varied manually, starting with $a=4$ (a sharp switchover); it yielded a shallow minimum in

χ^2 near $a=1$ and was frozen at that value in further computations. Again, the absolute minimum with respect to v_S was achieved near $v_S=16$, so that value was also fixed in further fitting. It is noteworthy that G_v is 66% of the well depth at $v=16$, so this result is consistent with our earlier observations about the optimal choice of v_S.

Both approaches, MXC and MXS, achieved significant lowering of chi-square from the NDE fit of Appadoo *et al.*[16]—by about 24% and 28%, respectively. [For reference, the relative statistical error in chi-square is $(2/\nu)^{1/2}$, or 1.4% in the present case.] Band-by-band comparisons of the statistics for the Appadoo NDE and the MXR fits indicate that most of the gains of the latter are achieved in the low-v-region. These gains do come with a price: a greater number of parameters needed for the MXR fits (33 vs 25).[38] However, the information content is comparable, as shown by the number of decimal digits needed to convey the results adequately after rounding. For the MXR fits, that number is about 150 (see below), as compared with 250 reported in Ref. 16; but the NDE results from the latter study can be rounded more aggressively with no loss of reliability, using the round-and-refit approach,[39,40] again leading to a ~150-digit representation.

The results from both MXR fits were used to compute (1) the statistical errors in T_v and B_v; (2) RKR potential curves for the A state and their statistical error; and (3) from these RKR curves, the quantum-mechanical values of T_v, B_v, D_v, and H_v and their statistical errors.[33] These computations revealed (A) changes in T_v and B_v from the Appadoo *et al.* analysis that exceeded the statistical errors by an order of magnitude in some v regions; (B) smaller but still statistically significant differences between the T_v and B_v values from the two MXR fits; and (C) statistically significant changes in D_v and H_v from the Ref. 16 values. The CDC computations also revealed significant "noise" in the D_v and H_v values computed from the MXC results. This behavior is tentatively attributed to high-order discontinuities in the RKR potential curve stemming from discontinuities in T_v and B_v beyond the first derivative included in the constraints. This effect represents a limitation for the MXC approach in precise work. It did not occur in the MXS-based computations.

The changes in D_v and H_v are large enough to warrant adjustment and further iteration in the analysis of T_v and B_v. Although the primary purpose of the present work is to test the efficacy of mixed representations rather than to provide new constants for the A state,[41] it is still desirable to verify that errors in the CDCs are not responsible for artifactually low chi-square in the present fits. Accordingly, I have repeated the MXS analysis with iterative adjustment of the CDCs. After about 10 cycles the maximum cycle-to-cycle changes in the latter were all less than ~1 part in 10^4 (0.002% for D_v, rising to 0.1% for M_v), and the variance was actually 2% lower than that of the original MXS fit.[42] Rounded results of this fit are given in Table I. The changes in T_v, B_v, and the CDCs are illustrated in Figs. 3 and 4.

The statistical errors computed for G_v and B_v via Eq. (2), by propagating the error through the RKR and quantum computations, agree well with estimates computed directly from the fit parameters up to $v\approx 30$, beyond which the RKR curve was adjusted to maintain a smooth repulsive branch.[43] Similar results were observed for the D state of I_2 in Ref. 33. The statistical errors in Q_v (computed directly from the fit parameters), D_v, and H_v are illustrated in Fig. 5. The results for the latter two are commensurate with the observed stabil-

TABLE I. Spectroscopic parameters for the A state of I_2, from MXS fit with iterative adjustment of centrifugal distortion constants. Dissociation limit fixed at 12 547.354 cm^{-1} above the minimum of the X state (Ref. 16) making $\mathcal{D}_e=1639.904$ cm^{-1} for the A state. Switching v $(v_S)=16$.

Parameter[a]	Vibrational	Rotational[b]
$c_0(T_e/B_e)$	10 907.449 7 (33)	0.027 394 2 (5)
$c_1(\omega_e/\alpha_e)$	92.852 4 (63)	$2.694\ 27\ (819)\times10^{-4}$
c_2	−1.469 443 (4 322)	-8.62×10^{-6}
c_3	−0.017 53	$7.260\ 6\times10^{-7}$
c_4	$4.163\ 1\times10^{-4}$	-2.269×10^{-7}
c_5	$-4.862\ 3\times10^{-5}$	$3.259\ 637\times10^{-8}$
c_6	4×10^{-6}	-2.8×10^{-9}
c_7	-3.5×10^{-8}	1.366×10^{-10}
c_8		-2.9×10^{-12}
$X_{0/1}$[c]	0.005 96	7.66×10^{-4}
$v_{\mathcal{D}}/p_1$	55.634 (6)	−0.173 556
p_2	$-3.732\ 818\times10^{-3}$	0.013 841 34
p_3	$3.272\ 2\times10^{-4}$	$-7.386\ 731\ 4\times10^{-4}$
p_4	-1.537×10^{-5}	$2.283\ 5\times10^{-5}$
p_5	$4.156\ 061\times10^{-7}$	-3.77×10^{-7}
p_6	-6.054×10^{-9}	2.6×10^{-9}
p_7	3.7×10^{-11}	
σ^2 [d]	3.36×10^{-5}	

[a]Units cm^{-1} for polynomial coefficients and $X_{0/1}$, cm^{-2} for σ^2, dimensionless for others. All parameters have been rounded and refitted systematically to preserve their reliability. [39] Where given, figures in parentheses represent standard errors, in terms of final digits.

[b]Ω-doubling constant, $Q_v=11.2\times10^{-7}+7.3\times10^{-8}(v+1/2)+3.2\times10^{-9}(v+1/2)^2$. Coefficient of 7th-order CDC, $k_7=0.0383\ (6)$.

[c]X_0 and X_1 fixed at values given in Ref. 16.

[d]Estimated variance for measurements of unit weight. Assuming these have $\sigma=0.005$ cm^{-1}, [16] this gives reduced chi-square $\chi^2_\nu=1.34$.

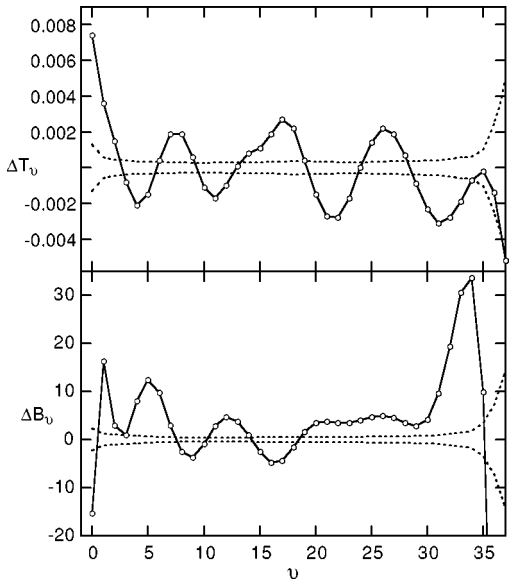

FIG. 3. Changes in T_v (cm^{-1}) and $B_v(10^{-7}$ $cm^{-1})$ from the analysis of Table I, and the statistical error band (dashed curves). The plotted quantities are the new values minus those of Ref. 16.

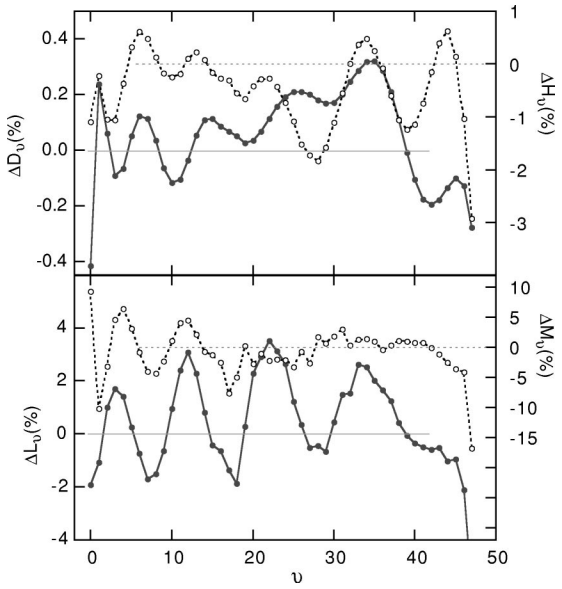

FIG. 4. Changes (%) in the first four CDCs, from the analysis of Table I. Plotted quantities are the new values minus those of Ref. 16. Note different scales for the two quantities plotted in each frame—solid points and lines for D_v and L_v.

ity of these quantities in the final cycles of the iterative refinement summarized in Table I and in fact served as a guideline in those calculations.

In the previous work, no effort was made to correct the RKR curves for their inherent semiclassical origin, so the systematic errors in the quantum computed G_v and B_v are also of interest. The values for the former were as much as 0.05 cm^{-1}, which is an order of magnitude greater than its statistical error. For B_v the systematic errors were less than 10^{-6} cm^{-1} below $v=30$, but this again exceeds the statistical error by more than an order of magnitude. Beyond $v=30$ the computed B_v drops off from the fitted value more strongly, as a direct consequence of the left-branch smoothing. The differences, which are too small to see on the scale of Fig. 1, are in a direction to improve agreement with the more recent estimates from Yukiya *et al.*,[23] though at $v=35$ the computed B_v still exceeds the estimate from the latter authors by 1.9×10^{-5} cm^{-1}. While this difference is probably significant, it is difficult to make quantitative comparisons with the results from Ref. 23, because the authors

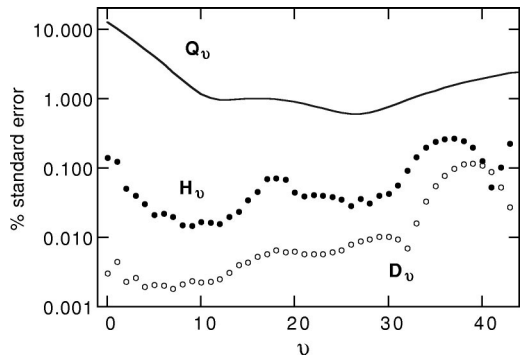

FIG. 5. Statistical errors in D_v, H_v, and Q_v from MXS analysis. Note the logarithmic ordinate.

reported only phenomenological CDCs for D_v and H_v, neglecting the contributions from higher-order terms, which are significant for their range of observed J.

The band-by-band statistical examination of the data mentioned earlier suggested that the R/P data from Ref. 16 are inferior in quality to the Q-only data; and even the latter seem to deteriorate in the high-v region. Also, some of the largest residuals among the fitted data belonged to lines that were multiply assigned. To check on the possible significance of these matters, I conducted an iterative analysis like that of Table I on a data set which had been edited for removal of 50 of the offending multiple assignments, with downweighting by a factor of four for all the R/P lines as well as the Q lines for $v>30$. These changes in the data set produced only minor changes in the spectroscopic constants. However, the fit variance was a factor of two smaller, suggesting that the high quality data from Ref. 16 are actually better ($\sigma=0.004$ cm^{-1}) than assumed there.[44]

IV. CONCLUSION

Mixed representations (MXRs)—polynomials in $(v+\frac{1}{2})$ for low v, near-dissociation expansions in (v_D-v) for high—have been tested in their ability to fit an extensive and precise data set for the A state of I_2. Smoothness in T_v and B_v was ensured by fitting with exactly satisfied constraints (MXC), and by use of a switching function (MXS). Both approaches yielded significantly lower χ^2 than achieved by the NDE previously reported for this data set,[16] though they required eight additional parameters. However, the parameters of the MXRs show much less mutual correlation, so fitting to an increased number of them presented no computational difficulties.

Mixed representations have the advantage of yielding directly the common physical parameters associated with both the low-v region and the dissociation region.[45] Further, since both parts of the MXR are of lower order than would be required to fit the data to either a pure polynomial or a pure NDE, they are ''safer'' for extrapolating across data gaps. In the present tests, the MXC approach yielded noisy computed D_v and H_v values. The constraints also were an inconvenience in the estimation of numerical derivatives required to propagate the fit error into the various computed properties. No such problems arose in the MXS approach, which also gave lower chi-square. Thus, the MXS method appears preferable for both its ease of application and its performance.

The use of MXRs for the A state of I_2 has changed the spectroscopic constants of observed levels by amounts that are appreciable in a statistical sense but small for most practical applications. The changes in T_v and B_v (Fig. 3) display an oscillatory behavior as a function of v. Some of this is likely due to representation error in the original CDCs, which were fitted to NDE s before incorporation in the fits to determine T_v and B_v. However, some is also probably due to the different orders of functions used to represent these quantities here and in Ref. 16, and may be an inevitable consequence of the approximation of highly smooth quantities by empirical polynomial-based functions. For the highest levels analyzed by Appadoo *et al.*,[16] there is a suggestion of

systematic error in the assignments, from the behavior of the spectroscopic constants and the RKR curve above $v=30$, and from comparison with the more recent results from Yukiya *et al.*[23] It will be interesting to see how these data respond to analysis by direct fitting to the *A*-state potential curve,[41] which will also avoid or greatly reduce some of the problems inherent in the RKR approach, like the semiclassical-quantum inconsistency and unsmoothness in the repulsive branch.

ACKNOWLEDGMENT

I thank Bob Le Roy for providing the data from Ref. 16 and for helpful comments, including the suggestion to use exact computed values of the CDCs rather than their fitted approximations in the iterative analysis of Table I.

[1] G. Herzberg, *Spectra of Diatomic Molecules* (Van Nostrand, Princeton, NJ, 1950).
[2] R. J. Le Roy, J. Chem. Phys. **52**, 2678 (1970).
[3] J. Tellinghuisen, M. R. McKeever, and A. Sur, J. Mol. Spectrosc. **82**, 225 (1980).
[4] F. Martin, R. Bacis, S. Churassy, and J. Vergès, J. Mol. Spectrosc. **116**, 71 (1986).
[5] R. J. Le Roy and W.-H. Lam, Chem. Phys. Lett. **71**, 544 (1980).
[6] J. W. Tromp and R. J. Le Roy, Can. J. Phys. **60**, 26 (1982).
[7] J. Tellinghuisen, J. Chem. Phys. **78**, 2374 (1983).
[8] G. W. King, N. T. Littlewood, and I. M. Littlewood, Chem. Phys. **81**, 13 (1983).
[9] J. W. Tromp and R. J. Le Roy, J. Mol. Spectrosc. **109**, 352 (1985).
[10] J. C. D. Brand, A. R. Hoy, S. M. Jaywant, and A. W. Taylor, J. Mol. Spectrosc. **123**, 84 (1987).
[11] K. J. Jordan, R. H. Lipson, N. A. McDonald, and R. J. Le Roy, J. Phys. Chem. **96**, 4778 (1992).
[12] J. Tellinghuisen, Can. J. Chem. **71**, 1645 (1993).
[13] R. J. Le Roy, J. Chem. Phys. **101**, 10217 (1994).
[14] C. Amiot, J. Vergès, and C. E. Fellows, J. Chem. Phys. **103**, 3350 (1995).
[15] J. O. Clevenger and J. Tellinghuisen, J. Chem. Phys. **103**, 9611 (1995).
[16] D. R. T. Appadoo, R. J. Le Roy, P. F. Bernath, S. Gerstenkorn, P. Luc, J. Vergès, J. Sinzelle, J. Chevillard, and Y. D'Aignaux, J. Chem. Phys. **104**, 903 (1996).
[17] D. T. Radzykewycz and J. Tellinghuisen, J. Chem. Phys. **105**, 1330 (1996).
[18] Y. M. Liu, D. Y. Chen, L. Li, K. M. Jones, B. Ji, and R. J. Le Roy, J. Chem. Phys. **111**, 3494 (1999).
[19] V. A. Alekseev, D. W. Setser, and J. Tellinghuisen, J. Mol. Spectrosc. **194**, 61 (1999).
[20] C. Linton, F. Martin, A. J. Ross, I. Russier, P. Crozet, A. Yiannopoulou, L. Li, and A. M. Lyyra, J. Mol. Spectrosc. **196**, 20 (1999).
[21] C. Amiot and J. Vergès, J. Chem. Phys. **112**, 7068 (2000).
[22] F. Martin, P. Crozet, A. J. Ross, M. Aubert-Frecon, P. Kowalczyk, W. Jastrzebski, and A. Pashov, J. Chem. Phys. **115**, 4118 (2001).
[23] T. Yukiya, N. Nishimiya, and M. Suzuki, J. Mol. Spectrosc. **182**, 271 (1997).
[24] J. Tellinghuisen and J. G. Ashmore, Chem. Phys. Lett. **102**, 10 (1983).
[25] J. G. Ashmore and J. Tellinghuisen, J. Mol. Spectrosc. **119**, 68 (1986).
[26] E. Hwang, P. J. Dagdigian, and J. Tellinghuisen, J. Mol. Spectrosc. **181**, 297 (1997).
[27] I was not able to succeed with this approach in reproducing the published NDE analysis of Ref. 16; rather, I had to code the derivatives in closed form and work in quadrupole precision.
[28] D. E. Deming, *Statistical Adjustment of Data* (Dover, New York, 1964).
[29] P. R. Bevington, *Data Reduction and Error Analysis for the Physical Sciences* (McGraw-Hill, New York, 1969).
[30] J. Tellinghuisen, J. Mol. Spectrosc. **179**, 299 (1996).
[31] J. Tellinghuisen, J. Phys. Chem. A **104**, 2834 (2000).
[32] J. Tellinghuisen, J. Phys. Chem. A **105**, 3917 (2001).
[33] J. Tellinghuisen, J. Mol. Spectrosc. (in press).
[34] W. H. Press, B. P. Flannery, S. A. Teukolsky, and W. T. Vetterling, *Numerical Recipes* (Cambridge University Press, Cambridge, U. K., 1986).
[35] J. Tellinghuisen, Adv. Chem. Phys. **60**, 299 (1985).
[36] J. Tellinghuisen, J. Mol. Spectrosc. **122**, 455 (1987).
[37] The ''bands'' in the data set from Ref. 16 are conveniently all-Q or all-R/P, so a $v'-v''$ band having both occurs as two separate bands, facilitating this observation.
[38] For the MXC fit, the number of free parameters is reduced by 4, due to the constraints; this is partly responsible for its higher χ^2. However, repeating the fit without the constraints dropped χ^2 only 2.3%, so the MXS fit is achieving further reduction through ''blending'' of the two representations of each function in the switchover region. The parameter count does not include v_S or the switching function parameter a.
[39] J. Tellinghuisen, J. Mol. Spectrosc. **137**, 248 (1989).
[40] R. J. Le Roy, J. Mol. Spectrosc. **191**, 223 (1998).
[41] A reanalysis of these data and those of Ref. 23 is being conducted by M. Mohammadi and R. J. Le Roy, using methods like those of Ref. 16 and also a direct potential-curve fitting approach. [J. Y. Seto, R. J. Le Roy, J. Vergès, and C. Amiot, J. Chem. Phys. **113**, 3067 (2000)].
[42] The computed CDCs in Ref. 16 were given as fitted expressions. To avoid possible representation error in the present calculations, the CDCs were not fitted to functions of v, but rather were simply read from and written to a file. The constant K_6 was left at the expression of Ref. 16, but the coefficient of the K_7 term (k_7) was adjusted.
[43] The repulsive branches of RKR curves flare in or out at high v and must be replaced by a suitable smooth extension, with concomitant adjustment of the attractive branch to preserve the potential width (Ref. 35). On average the *A* left branch is behaving as R^{-15} in the $v=20-31$ region, so an R^{-15} extension was attached near $v=29$ and 30.
[44] Eliminating the 50 multiply assigned lines (0.5% of the assigned lines) dropped the fit variance $\sigma_{y1}{}^2$ (the variance for data of unit weight [J. Tellinghuisen, J. Mol. Spectrosc. **165**, 255 (1994)] from 3.36 to 3.15 $\times 10^{-5}$ cm^{-2}. Downweighting the R and P lines (1284 lines, or 13.4% of the assignments) dropped σ_{y1}^2 to 2.00×10^{-5} cm^{-2}, and downweighting in addition the Q assignments for $v>30$ (551 lines, or 5.8%) further lowered it to 1.72×10^{-5} cm^{-2}.
[45] With $a=1$ in Eq. (12), the lead polynomial coefficients are not *quite* the desired ''equilibrium'' values. For example, the contribution from the long-range part of the MXR for T_v amounts to about 0.0004 cm^{-1} at $v=-\frac{1}{2}$, 0.001 cm^{-1} at $v=1$, and 0.016 cm^{-1} at $v=5$, while that for B_v contributes 7×10^{-8} cm^{-1} at $v=1$ and 7×10^{-7} cm^{-1} at $v=5$.